https://doi.org/10.5194/egusphere-2026-6563
Preprint. Discussion started: 5 November 2026
© Author(s) 2026. CC BY 4.0 License.

Antecedent rainfall patterns and situational vulnerability of victims of rainfall-induced fatal landslides in Pakistan

Shibiao Bai[1] · Wenxin Zhu[1] · Xiu Wang[1] · Pinggen Zhou*[2]

[1] School of Marine Science and Engineering, State Key Laboratory of Climate System Prediction and Risk Management, Nanjing Normal University, Nanjing 210023, China

[2] China Institute of Geo-Environment Monitoring, Beijing, China

Correspondence: Pinggen Zhou (bjzhoupg@126.com)

Abstract: Fatalities from rainfall-induced landslides depend not only on rainfall conditions but also on the time of occurrence, the exposure setting and demographic vulnerability. In data-scarce mountain regions such as Pakistan, event-scale rainfall histories and individual casualty records have long been disconnected. This study places event-scale rainfall and individual victim circumstances within a single event catalogue, characterises antecedent rainfall patterns and tests whether they explain fatality magnitude, in order to inform scenario-based early warning in data-scarce mountains. Based on a 2004–2024 catalogue of rainfall-induced fatal landslides in Pakistan (positioned as a lower-bound estimate because flood–landslide–debris-flow–building-collapse cascades mask landslide-attributed deaths), 213 of 250 events with spatial accuracy levels I–II were matched to CHIRPS 0.05° daily rainfall, and individual attributes of 309 fatalities during 2018–2024 were compiled. Results show that 53.5% of events have zero event-day rainfall in CHIRPS; among four antecedent-rainfall types defined by event-day and 7-day antecedent rainfall, the low-event-day-rainfall types C and D together account for 86.4%, and sensitivity tests using 15/40, 20/50 and 25/60 mm boundaries give 81.2–89.7%, indicating robustness to the classification boundaries. The intensity–duration quantile relations share a common exponent of −0.59, yet no rainfall metric correlates significantly with per-event fatality. Victim records show that 66.0% of deaths with known setting occurred indoors and 74.5% of those with known timing occurred at night, making the night–indoor combination the most concentrated exposure; both gender and age are significantly associated with exposure setting ($\chi^2 = 28.61$, Cramér's $V = 0.367$; $\chi^2 = 35.34$, $V = 0.362$; $p < 0.001$), and the setting–timing association is also significant ($\chi^2 = 70.87$, $df = 2$, $p < 0.001$, $V = 0.594$). Rainfall therefore characterises the hydro-meteorological background of slope instability, whereas fatality consequences additionally depend on timing, exposed space and demographic attributes. Early-warning systems should consider both short-duration and antecedent cumulative rainfall, and translate warnings into scenario-based actions such as night-time evacuation of dwellings, mountain road control and management of children's activity spaces.

https://doi.org/10.5194/egusphere-2026-6563
Preprint. Discussion started: 5 November 2026
© Author(s) 2026. CC BY 4.0 License.

Keywords: rainfall-induced fatal landslide; antecedent rainfall; intensity–duration relation; exposure setting; social vulnerability; Pakistan

1 Introduction

Climate change is modifying short-duration intense rainfall and compound wetting sequences, introducing new uncertainty into rainfall-induced landslide risk across High Mountain Asia (Gariano and Guzzetti, 2016; Kirschbaum et al., 2020). Within this context, the Global Landslide Catalogue (GLC) compiled by Kirschbaum et al. (2010; 2015) from media reports and disaster databases, and the catalogue of deadly geohazards in China for 2013–2019 by Huang et al. (2022), provide both a methodological paradigm and a comparable benchmark for characterising fatal landslides at the event scale.

At the level of risk assessment and mechanism, Guzzetti (2000) provided an early quantification of landslide fatality risk in Italy, laying the foundation for vulnerability frameworks; Corominas et al. (2014) further set out recommendations for the quantitative analysis of landslide risk. The physical mechanism of rainfall-triggered landslides has been systematically elucidated: rainfall infiltration raises pore-water pressure and reduces effective stress, and failure occurs once the shear stress on the potential slip surface exceeds its strength, with failure able to lag the rainfall peak by several hours to several days (Iverson, 2000). The intensity–duration (I–D) threshold is a central framework, and the rainfall control of shallow landslides and debris flows has been continuously updated (Caine, 1980; Guzzetti et al., 2008). Regional studies show that about 85% of fatal landslides in Nepal occur during the June–September monsoon (Petley et al., 2007), that China exhibits a bimodal structure with a July–August main peak and an April–May secondary peak (Lin and Wang, 2018; Zhang et al., 2023), that Türkiye is most frequent during persistent winter rainfall (Görüm and Fidan, 2021), and that long-term Japanese data show a marked decline in landslide fatalities (Shinohara and Kume, 2022), indicating that different climatic systems shape the temporal pattern in distinct ways. Spatially, fatal landslides are strongly clustered along mountain-range orientations, windward rainfall belts and transport-corridor exposure zones (Sepúlveda and Petley, 2015; Haque et al., 2016). Notably, about 30% of rainfall-induced landslides worldwide show zero rainfall on the event day at daily resolution (Mirus et al., 2020; Emberson et al., 2022), showing that characterising triggering conditions by event-day rainfall alone easily overlooks the antecedent wetness background; moreover, the gender gap in disaster mortality widens with social inequality (Neumayer and Plümper, 2007).

https://doi.org/10.5194/egusphere-2026-6563
Preprint. Discussion started: 5 November 2026
© Author(s) 2026. CC BY 4.0 License.

However, the path from rainfall to death is not a linear causal chain. Similar rainfall histories can produce very different casualty magnitudes, because whether a slope failure enters a settlement, a road or an outdoor activity space, and whether people are asleep, in transit or in a low-coping-capacity state, determines whether a hazard turns into a disaster. Recent work has begun to move from simply counting fatalities towards explaining how physical exposure and social capacity shape unequal outcomes (Pollock and Wartman, 2020; Li et al., 2026). Cross-analyses of victim gender, age and circumstance have likewise demonstrated that disaster losses are strongly setting-dependent (Salvati et al., 2018; Sultana, 2020).

At the methodological level, the way antecedent rainfall is represented substantially affects threshold results: fixed accumulation windows, decay-weighted indices and complete rainfall events each emphasise different aspects of the slope wetness background and of the triggering condition (Crozier, 1999; Glade et al., 2000; Bai et al., 2013). At the same time, gridded and satellite precipitation products such as CHIRPS are widely used in regional landslide studies, yet product-specific biases and limited representation of local intense rainfall can shift numerical thresholds and weaken forecast skill (Brunetti et al., 2018; Chikalamo et al., 2020; Wang et al., 2021); thresholds should therefore be regarded as conditional on the chosen precipitation input, and their values are difficult to transfer directly between products. These methodological issues are particularly acute in data-scarce mountain regions such as Pakistan, and they further indicate that characterising triggering conditions by event-day rainfall or a single accumulation window alone easily misses the antecedent wetness background.

Northern Pakistan lies at the junction of the Himalaya, the Karakoram and the Hindu Kush, where tectonic activity is intense and relief is high, and where the monsoon and western disturbances jointly shape a complex rainfall rhythm. Mountain settlements and transport corridors concentrate along steep river valleys, so that natural hazard and human exposure overlap strongly. Existing national-scale studies mostly rely on rainfall data at coarse temporal resolution, rarely perform event-by-event rainfall extraction under explicit spatial-accuracy constraints, and lack analyses that connect the triggering process with individual victim records (Shabbir et al., 2023). In particular, the analysis of fatal landslides in Pakistan for 2003–2019 by Shabbir et al. (2023) was likewise based solely on monthly TRMM rainfall, without event-specific, multi-window rainfall extraction or triggering-pattern classification for fatal landslides; in addition, effective coverage of Pakistan by the Unified Global Landslide Catalogue (UGLC) ends in 2017, so that events after 2018 must be filled in by independent multi-source compilation. These gaps remain pronounced in terms of long time series, high spatial accuracy and event–individual linkage. Existing research broadly follows three relatively independent lines. The first analyses the spatiotemporal distribution of events, fatalities and triggers using national or global fatal-landslide catalogues (Petley, 2012; Froude and Petley,

https://doi.org/10.5194/egusphere-2026-6563
Preprint. Discussion started: 5 November 2026
© Author(s) 2026. CC BY 4.0 License.

2018; Sultana, 2020; Shabbir et al., 2023; Zhang et al., 2023). The second characterises the hydro-meteorological conditions of landslide occurrence from rainfall infiltration mechanisms and rainfall intensity–duration relations (Caine, 1980; Iverson, 2000), with some studies further discussing the potential influence of climate change and changing extreme rainfall on rainfall-induced landslide activity (Gariano and Guzzetti, 2016; Kirschbaum et al., 2020). The third uses individual-level fatality records to analyse the influence of gender, age, behaviour, buildings and circumstance on human vulnerability (Salvati et al., 2018; Pollock and Wartman, 2020). These lines have respectively advanced understanding of landslide occurrence conditions and of human fatality consequences, but studies that systematically link event-scale rainfall histories with individual victim circumstances within a single event database remain scarce. How different rainfall backgrounds co-occur with exposure settings such as night-time dwellings, mountain transport and outdoor activity, and whether rainfall metrics can explain the fatality magnitude of an individual event, therefore remain open questions. At larger scales, the risk of fatal landslides on world mountains is highly concentrated in developing regions and governed by socio-economic factors such as wealth and land-cover change (Fidan et al., 2026); in data-scarce mountain areas such as northern Pakistan, systematic landslide cataloguing and vulnerability mapping remain inadequate (Ullah et al., 2024), and the event-specific approach under spatial-accuracy constraints adopted here responds directly to that gap. Comparable national-scale analyses of fatal-landslide spatiotemporal patterns exist for Türkiye (Görüm and Fidan, 2021), suggesting that these regularities are shared to some degree among mountain-front countries.

Drawing on the shift in research focus from “the amount of loss” to “the mechanism by which loss is produced”, this paper addresses three questions: (1) What are the respective characteristics of event-day rainfall and antecedent cumulative rainfall, and does a single standard triggering pattern exist? (2) What intensity–duration quantile relations characterise the fatal-landslide sample, and are rainfall metrics at different timescales significantly associated with the fatality magnitude of an individual event? (3) How is the triggering pattern transmitted through timing and exposure setting to different age and gender groups?

2 Study area and methods

2.1 Study area and analysis sample

Pakistan lies between 23°35′–37°05′ N and 60°50′–77°50′ E; the northern mountains are the main concentration of rainfall-induced fatal landslides (Fig. 1). The catalogue compiled in this study contains 250 events and 2073 fatalities, of which 96 are of accuracy level I and 117 of level II, giving 213 events entering the event-by-event

https://doi.org/10.5194/egusphere-2026-6563
Preprint. Discussion started: 5 November 2026
© Author(s) 2026. CC BY 4.0 License.

rainfall analysis. The individual-level subset for 2018–2024 contains 309 victims, with identifiable counts of 212 for gender, 270 for age group, 300 for setting and 204 for time of day.

Climatologically, Pakistan lies at the northwestern margin of the South Asian monsoon domain, and precipitation is controlled by two synoptic systems: the Indian Ocean southwesterly monsoon from June to September, which frequently produces concentrated heavy rainfall in the northern mountains, and the western disturbances arriving from the Mediterranean–West Asian sector between December and April, which bring persistent rainfall and snowfall; their superposition produces a complex bimodal seasonal rhythm. Geologically, the north lies at the leading edge of the India–Eurasia collision zone, where major structures such as the Main Boundary Thrust (MBT) and the Main Central Thrust (MCT) control rock-mass structure and slope stability (Champati ray et al., 2007). Over the past two decades the population of Pakistan grew from about 155 million in 2004 to about 245 million in 2024; settlements in the northern mountains expanded along valley floors, slope foots and gully mouths, and the exposure of people and property increased steadily (Haque et al., 2019). The first-order administrative units comprise Khyber Pakhtunkhwa (KP), Azad Jammu and Kashmir (AJK), Gilgit-Baltistan (GB), Punjab, Balochistan, Sindh and the Islamabad Capital Territory. This study uses the most recent district-level boundaries published by the Humanitarian Data Exchange (HDX) as the spatial-statistical baseline.

https://doi.org/10.5194/egusphere-2026-6563
Preprint. Discussion started: 5 November 2026
© Author(s) 2026. CC BY 4.0 License.



Fig. 1. Location, topography and administrative divisions of the study area in Pakistan. The inset shows the position of Pakistan in Asia. Base-map sources are indicated within the figure.

Table 1. Data sets and analysis samples.

Data level	Time span	Sample size	Main variables	Role
Full event catalogue	2004–2024	250 events / 2073 fatalities	Location, date, fatalities, accuracy	Overall context
Rainfall analysis subset	2004–2024	213 events	P0, AP3, AP7, AP15, AP30	Triggering-pattern and I–D analysis
Individual victim subset	2018–2024	309 individuals	Gender, age, setting, time of day	Vulnerability and cascade analysis

2.2 Catalogue construction and quality control

Events for 2004–2017 were screened from the Unified Global Landslide Catalogue, and those for 2018–2024 were supplemented through news reports, government bulletins and international databases. An event was included only if it simultaneously satisfied three conditions: a rainfall-related trigger, an identifiable slope mass movement, and direct human fatalities; multi-hazard processes such as floods and building collapses were included only where

https://doi.org/10.5194/egusphere-2026-6563
Preprint. Discussion started: 5 November 2026
© Author(s) 2026. CC BY 4.0 License.

landslide evidence existed. Events were cross-checked and de-duplicated using date, location and casualty information. Spatial accuracy is graded into level I (location error < 5 km), level II (5–50 km) and level III (> 50 km); only levels I–II enter the gridded rainfall matching. Here we retain only the accuracy-grading conventions directly relevant to gridded rainfall extraction, and, given the multi-hazard masking effect, we position the catalogue as a lower-bound estimate of rainfall-induced fatal landslides.

It is worth noting that in years of heavy rainfall (e.g. 2010 and 2022), landslides, debris flows, flash floods and building collapses frequently occur concurrently, and authoritative agencies often aggregate deaths into macro-level categories such as “flood/rainstorm-related deaths”, so that deaths directly attributable to landslides are systematically masked in macro statistics (multi-hazard masking effect). Accordingly, this catalogue includes only events with explicit evidential support that can be confirmed as rainfall-triggered and as causing death directly by landslide, and positions the result as a lower-bound estimate of rainfall-induced fatal landslides, thereby maintaining high confidence and low noise along the causal chain “rainfall → landslide → death”.

Event definition follows the updated Varnes classification (Hungr et al., 2014), including landslides, debris flows, rock falls and composite slope movements; only the rainfall trigger class is retained, determined through textual evidence, contextual interpretation and posterior meteorological verification, with seismic, anthropogenic and pure snowmelt events excluded. The base layer is the Unified Global Landslide Catalogue (UGLC) (Mancino et al., 2026), and the gap for 2018–2024 was filled by cross-verified compilation from news reports, government bulletins and international databases.

2.3 Rainfall data and metrics

Rainfall is taken from the CHIRPS v2.0 daily product at 0.05° spatial resolution (Funk et al., 2015), extracted by event coordinates on Google Earth Engine for the day of occurrence and the preceding 30 days. P0 is the event-day rainfall; AP3, AP7, AP15 and AP30 are the cumulative rainfall over the 3, 7, 15 and 30 days preceding the event; Total_7d is the 7-day total rainfall including the event day. All statistics are computed per event. Rainfall extraction was implemented on the Google Earth Engine cloud platform (Gorelick et al., 2017), taking the CHIRPS daily series at the event coordinate point; to avoid location error, event-by-event meteorological extraction was performed only for level I–II events (n = 213). In addition to P0, AP3, AP7, AP15 and AP30, Total_7d is also computed to partly offset the effects of day-boundary misalignment and of the smoothing of local intense convection.

https://doi.org/10.5194/egusphere-2026-6563
Preprint. Discussion started: 5 November 2026
© Author(s) 2026. CC BY 4.0 License.

It should be noted that CHIRPS is a satellite–gauge merged gridded precipitation product, and its spatial resolution (0.05°) and product biases may smooth local convective extremes in mountains; the rainfall metrics and thresholds extracted from it are therefore numerically dependent on this input product (Brunetti et al., 2018; Chikalamo et al., 2020; Wang et al., 2021). Existing evaluations show that, even with systematic biases, satellite precipitation products retain discriminative ability in characterising triggering conditions (Wang et al., 2021); this study therefore describes the triggering background through the combination of event-day and multi-window antecedent rainfall, and interprets low P0 values with caution (Sect. 4).

2.4 Triggering-pattern classification and seasonal division

To describe the combined characteristics of event-day rainfall and antecedent cumulative rainfall, we adopt P0 = 20 mm and AP7 = 50 mm as the baseline classification boundaries. In the sample both P0 and AP7 are right-skewed, with 20 mm corresponding approximately to the 86th percentile of the empirical P0 distribution and 50 mm close to the 70th percentile of the empirical AP7 distribution. These two round values are chosen to distinguish, within the bulk of the sample, events with relatively high event-day rainfall from those with relatively high antecedent cumulative rainfall. The boundaries are used only for within-sample scenario classification and group comparison; they do not represent physical triggering thresholds for slope instability and are not intended for operational warning. According to the values of P0 and AP7 relative to the baseline boundaries, events are classified into four types: type A = high P0–high AP7, type B = high P0–low AP7, type C = low P0–high AP7, and type D = low P0–low AP7. Strictly greater than the corresponding boundary defines a high value, and equal to or below it defines a low value. The classification boundaries (P0 = 20 mm, AP7 = 50 mm) serve within-sample scenario identification and group comparison and do not represent an absolute triggering lower limit; their setting refers to the magnitude range of I–D threshold studies for shallow landslides (Caine, 1980; Guzzetti et al., 2008) and is determined together with the quantile distribution of the present sample. The lag effect of antecedent rainfall on instability has been confirmed by slope moisture monitoring (Mirus et al., 2020), so type C (weak immediate cause + strong antecedent) typically reflects saturation–delayed triggering.

To assess the sensitivity of the classification to the choice of boundaries, the classification was repeated with three sets of P0/AP7 combinations — 15/40, 20/50 and 25/60 mm — and the numbers of type A–D events and the combined share of types C and D were compared across schemes. The sensitivity analysis is mainly used to test whether the conclusion that “low event-day-rainfall types dominate” remains consistent after reasonable adjustment of the classification boundaries.

https://doi.org/10.5194/egusphere-2026-6563
Preprint. Discussion started: 5 November 2026
© Author(s) 2026. CC BY 4.0 License.

2.5 Intensity–duration quantile relations

For windows of D = 1, 3, 7, 15 and 30 days, the corresponding cumulative rainfall is divided by D to obtain the mean intensity I (mm d^{-1}); after removing observations with $I \leq 0$, $I = aD^{\gamma}$ is fitted in double-logarithmic space. A common slope $\gamma = -0.59$ is first estimated, and then the 10th, 50th and 90th percentile intercepts are estimated to obtain three parallel curves. This method describes severity levels within the sample and is not given a causal interpretation (Saha and Bera, 2024). The correlation between rainfall metrics and fatality magnitude is tested with Spearman rank correlation (Spearman, 1904), which is robust to skewed distributions and extreme values. To avoid the limitation of a single a priori window, we also compute several antecedent windows — AP3, AP7, AP15 and AP30 — and systematically compare the representational ability of antecedent rainfall over different periods (Ning et al., 2023), rather than relying on a single pre-set timescale.

2.6 Victim variables and statistical analysis

Individual variables comprise gender (male/female/unknown), age group (< 15, 15–60, > 60 years/unknown), setting (indoor/transport/outdoor/unknown) and time of day (daytime/night/unknown). Descriptive statistics retain the "unknown" category to present data completeness, whereas cross-tabulations and tests use complete cases with all relevant fields known. Because only three victims were elderly, the age chi-square test merges them with the 15–60 group into adults (≥ 15 years). Group comparisons of continuous variables use the two-sided Mann–Whitney U test; the relation between rainfall and fatality count uses two-sided Spearman rank correlation; categorical variables are tested with the Pearson chi-square test, and Cramér's V is reported. The significance level is set at 0.05. Analysis and plotting were performed with Python and R.

2.7 Construction of the triggering background–exposure setting pathway

Individual records are linked to the 213 rainfall events through Event_ID and organised into five dimensions in sequence: triggering pattern, time of day, setting, age and gender. Only the 145 individuals for whom all five fields are explicit are retained, and frequencies are aggregated by complete combination path. Band width is proportional to the number of individuals, and colours are kept consistent along the triggering pattern. This visualisation shows the co-occurrence structure; it is not used to estimate transition probabilities or causal effects.

https://doi.org/10.5194/egusphere-2026-6563
Preprint. Discussion started: 5 November 2026
© Author(s) 2026. CC BY 4.0 License.

3 Results

3.1 Multi-scale rainfall background and zero event-day rainfall

The rainfall metrics of the 213 events are all markedly right-skewed (Fig. 2; Table 2). The median P0 is 0 mm and the mean is 10.3 mm; the medians of AP7 and AP30 are 27.0 and 100.0 mm, respectively. As the accumulation window lengthens the distribution shifts towards higher values overall, but the dispersion increases at the same time, reflecting substantial differences among events between short-term pulses and long-term wetness backgrounds.

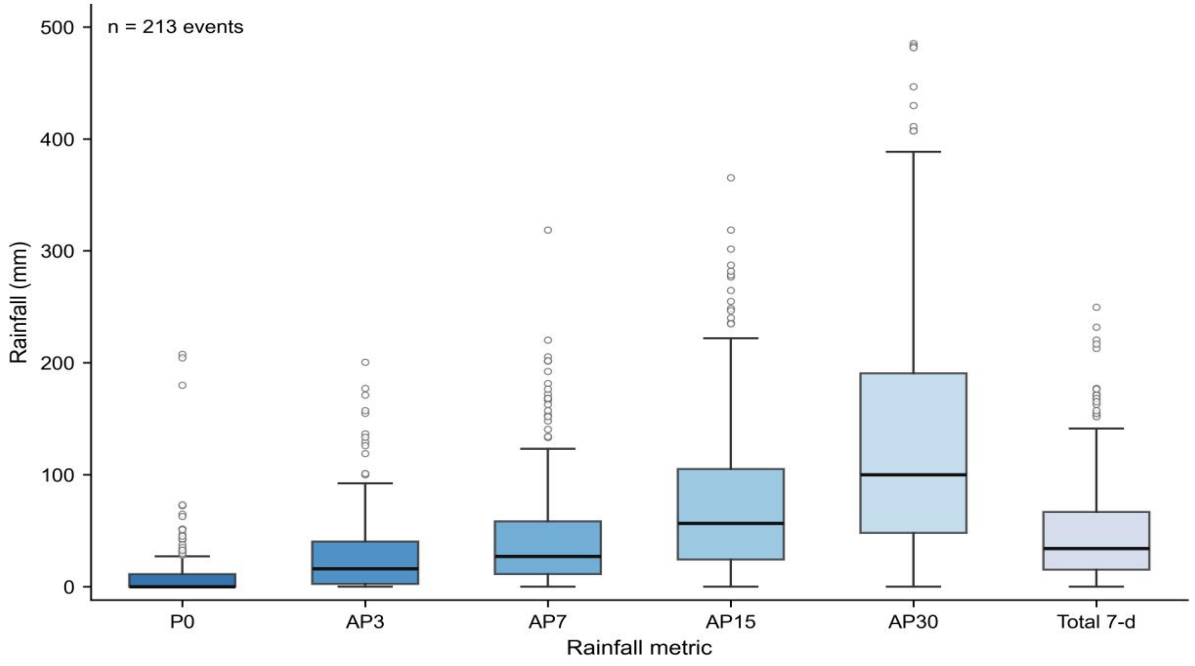


Fig. 2. Distribution of multi-timescale rainfall metrics for 213 fatal landslide events. Boxes show the interquartile range, the centre line the median, and points the individual event observations.

Table 2. Descriptive statistics of rainfall metrics (n = 213).

Metric	Min	25th pct	Median	Mean	75th pct	Max	SD
P0	0	0	0	10.3	11.2	207.6	26.3
AP3	0	2.4	16.0	28.3	40.4	200.5	36.3
AP7	0	11.3	27.0	45.0	58.4	318.5	52.4
AP15	0	24.3	56.7	76.7	105.1	365.2	72.8
AP30	0	48.1	100.0	135.0	190.5	485.1	115.2
Total_7d	0	15.1	34.1	50.4	66.7	249.6	52.0

https://doi.org/10.5194/egusphere-2026-6563
Preprint. Discussion started: 5 November 2026
© Author(s) 2026. CC BY 4.0 License.

Note: all units are mm. P0 is event-day rainfall; APn is the cumulative rainfall over the n days preceding the event.

A total of 114 events (53.5%) have P0 = 0. The median AP7 is 27.46 mm for the P0 = 0 group and 25.89 mm for the P0 > 0 group, and the median AP30 is 91.32 and 109.64 mm, respectively; the Mann–Whitney tests are not significant in either case (AP7: p = 0.523; AP30: p = 0.526; Fig. 3). This result should not be interpreted as the two groups having identical slope states; rather, it shows that "no rain on the event day" at daily and 5 km resolution does not exclude an antecedent rainfall influence. Time-zone day boundaries, errors in event dates, spatial averaging of local convection and delayed failure can all produce low P0 values.

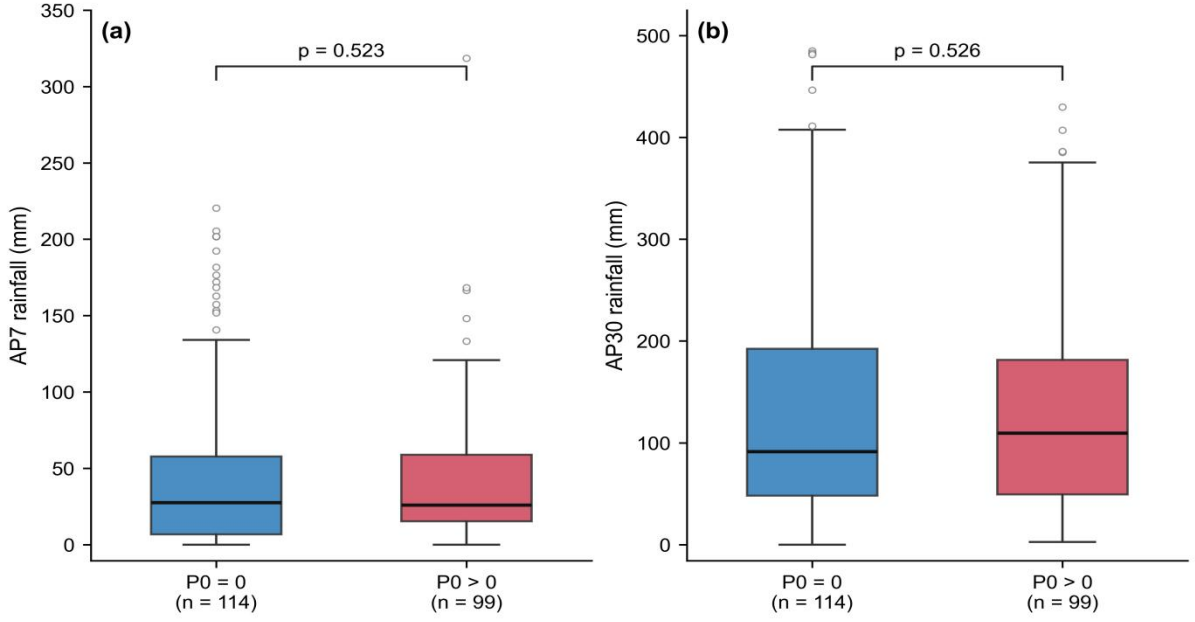


Fig. 3. Comparison of antecedent cumulative rainfall between events with P0 = 0 and P0 > 0. Values in brackets are two-sided Mann–Whitney test p values.

3.2 Four antecedent rainfall patterns and their seasonal preferences

Using P0 = 20 mm and AP7 = 50 mm as the baseline classification boundaries, the 213 events are classified into four types A–D (Fig. 4; Table 3). Type D (low P0, low AP7) is the most frequent, with 132 events (62.0%); type C (low P0, high AP7) has 52 events (24.4%); types A (high P0, high AP7) and B (high P0, low AP7) have 12 (5.6%) and 17 (8.0%) events, respectively. Types C and D together comprise 184 events, or 86.4%, indicating that low-P0 types dominate the sample under the baseline scheme. The sensitivity analysis shows that with the 15/40 mm boundaries the numbers of types A, B, C and D are 18, 22, 58 and 115, with C + D at 81.2%, and with the 25/60

https://doi.org/10.5194/egusphere-2026-6563
Preprint. Discussion started: 5 November 2026
© Author(s) 2026. CC BY 4.0 License.

mm boundaries the four types number 9, 13, 44 and 147, with C + D at 89.7%. Thus, under all three schemes (15/40, 20/50 and 25/60 mm), the low-P0 types C + D account for more than 81%, indicating that the core conclusion that low event-day-rainfall types dominate is robust to reasonable adjustment of the classification boundaries. Under the baseline scheme, type B accounts for only 8.0% of events but caused 185 deaths in total, with a mean of 10.9 deaths per event, the highest among the four types; this difference is descriptive only and cannot be attributed solely to event-day rainfall intensity.

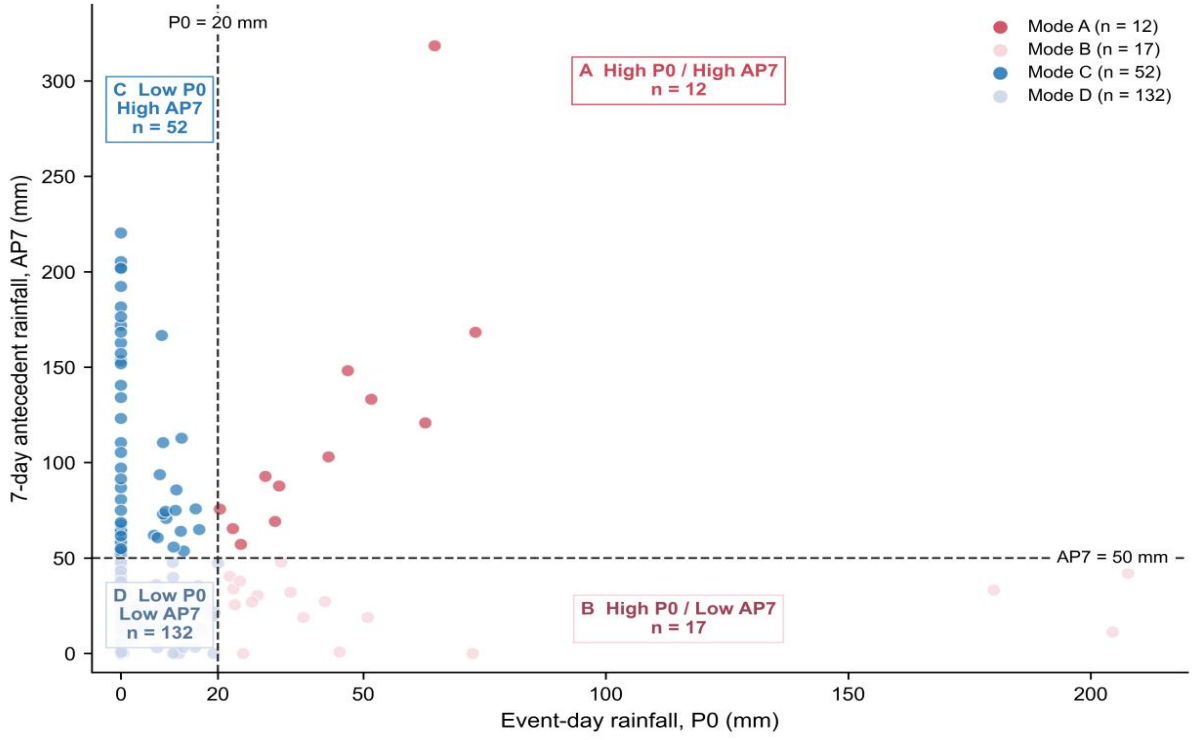


Fig. 4. Four rainfall-background types defined by event-day rainfall P0 and 7-day antecedent rainfall AP7. Dashed lines show the sample classification boundaries of 20 mm and 50 mm, and point size indicates the number of fatalities per event. These boundaries are used for within-sample classification and do not represent physical triggering thresholds.

Table 3. Events and fatalities by triggering-pattern type.

Type	Criterion	Events	Share	Fatalities	Mean fatalities per event
A	High P0 + high AP7	12	5.6%	74	6.2
B	High P0 + low AP7	17	8.0%	185	10.9
C	Low P0 + high AP7	52	24.4%	374	7.2
D	Low P0 + low AP7	132	62.0%	999	7.6

https://doi.org/10.5194/egusphere-2026-6563
Preprint. Discussion started: 5 November 2026
© Author(s) 2026. CC BY 4.0 License.

Note: high P0 means P0 > 20 mm and high AP7 means AP7 > 50 mm; values equal to the boundary are assigned to the low group.

Seasonal composition further shows that types A + B account for 20.0% in the monsoon season, higher than the 5.0% in the pre-monsoon season; the winter share is 14.3%, and all 11 post-monsoon events belong to type D (Fig. 5). In all seasons, however, types C + D remain dominant, indicating that high immediate rainfall and antecedent wetness are not mutually exclusive but occur in different proportions across seasons.

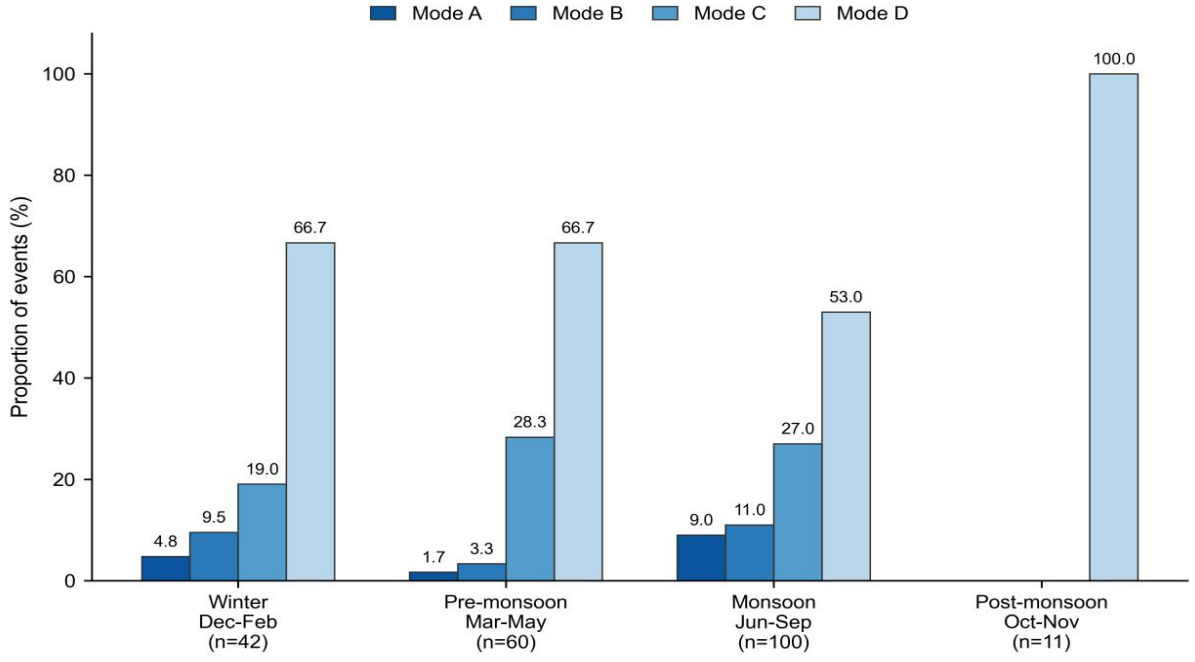


Fig. 5. Composition of triggering-pattern types A–D by season. Numbers within each bar give the event count or proportion of the corresponding type, and colour shading distinguishes the types.

3.3 Intensity–duration quantile relations and their relation to fatality magnitude

Mean rainfall intensity was computed for the 1, 3, 7, 15 and 30 day windows, and three quantile relations with a common slope of −0.59 were obtained in double-logarithmic space (Fig. 6): $I = 5.45D^{-0.59}$ at the 10th percentile, $I = 17.96D^{-0.59}$ at the 50th percentile and $I = 60.48D^{-0.59}$ at the 90th percentile. As duration increases, the mean intensity required to reach a given quantile level decreases, consistent with the empirical understanding that prolonged wetting progressively reduces slope stability. These curves describe the conditional distribution of rainfall intensity at different durations within the fatal-event sample; they are not used to discriminate triggered from non-triggered conditions, nor do they represent independently validated operational warning thresholds.

https://doi.org/10.5194/egusphere-2026-6563
Preprint. Discussion started: 5 November 2026
© Author(s) 2026. CC BY 4.0 License.

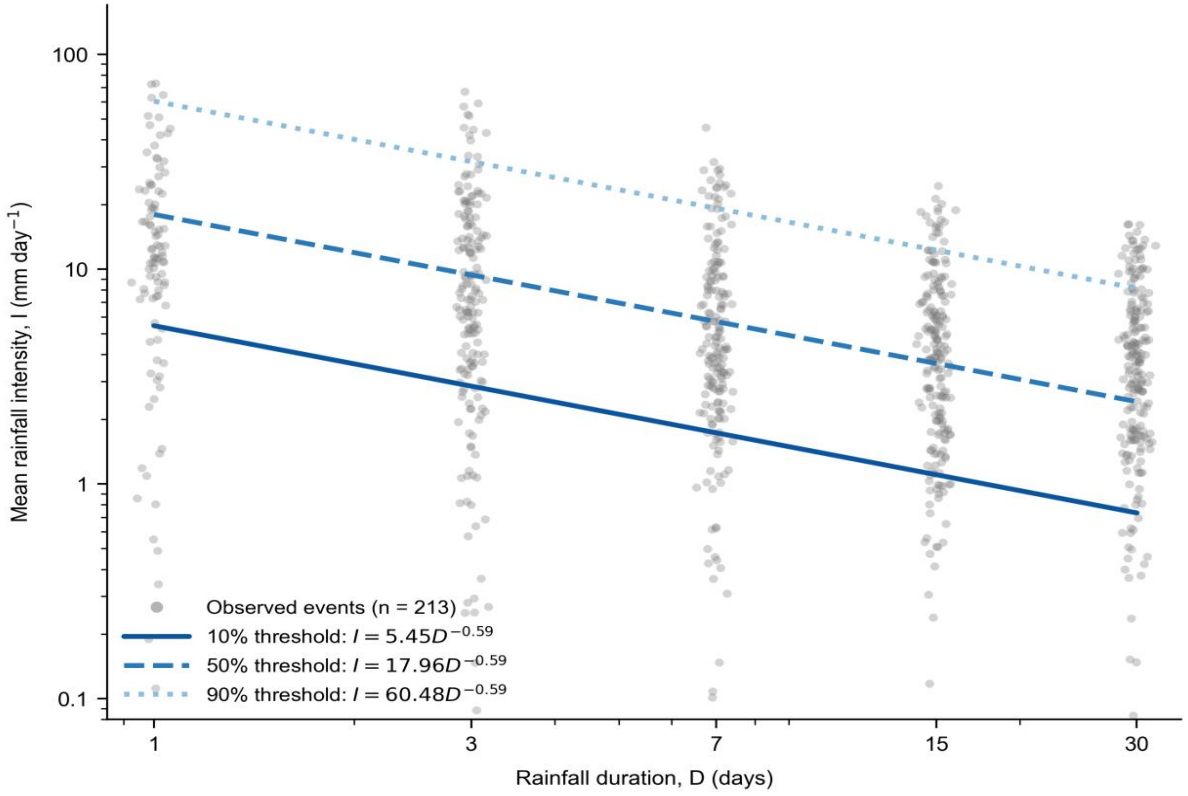


Fig. 6. Rainfall intensity–duration quantile relations for the sample of rainfall-induced fatal landslide events in Pakistan. Grey points are positive rainfall observations, and the three blue curves show the 10th, 50th and 90th percentile relations.

At the same time, the Spearman correlations between P0, AP3, AP7, AP15, AP30 and Total_7d and the number of fatalities per event are all non-significant (Table 4). The largest absolute correlation coefficient is that of AP3 (ρ = 0.103, p = 0.133), which is still weak and does not reach statistical significance. Rainfall metrics therefore help to describe the triggering environment, but they cannot replace analysis of population exposure, building conditions, activity timing and transport location.

Table 4. Spearman correlations between rainfall metrics and fatalities per event.

Metric	ρ	p value	Interpretation
P0	−0.015	0.825	Not significant
AP3	0.103	0.133	Not significant
AP7	0.073	0.292	Not significant
AP15	0.052	0.448	Not significant
AP30	−0.038	0.581	Not significant
Total_7d	0.088	0.203	Not significant

Note: two-sided tests; significance level $\alpha = 0.05$.

https://doi.org/10.5194/egusphere-2026-6563
Preprint. Discussion started: 5 November 2026
© Author(s) 2026. CC BY 4.0 License.

3.4 Victim setting, timing and demographic structure

Among the 309 victims, the setting is identifiable for 300: indoor 198 (66.0%), transport 62 (20.7%) and outdoor 40 (13.3%). Time of day is identifiable for 204, of whom 152 (74.5%) died at night. Among the 201 victims with both setting and time of day known, the night–indoor combination accounts for 115 individuals, or 92.0% of the valid indoor sample, whereas daytime–outdoor accounts for 24. The association between setting and time of day is significant ($\chi^2 = 70.87$, df = 2, $p < 0.001$, Cramér's V = 0.594).

Among the 212 victims with identifiable gender and explicit setting, males account for 92.2% of transport deaths and 70.3% of outdoor deaths, while indoor deaths are split evenly between males and females at 50.0% each; gender and setting are significantly associated ($\chi^2 = 28.61$, df = 2, $p < 0.001$, V = 0.367). In the age analysis, the elderly group of only three individuals was merged with the 15–60 group into adults (≥ 15 years) to satisfy the expected-frequency requirement of the Pearson chi-square test. Among the 269 valid cases, adults account for 96.8% of transport deaths, children for 44.9% of indoor deaths and 40.0% of outdoor deaths; age and setting are significantly associated ($\chi^2 = 35.34$, df = 2, $p < 0.001$, V = 0.362; Table 5).

Table 5. Cross-structure of fatality setting with time of day, gender and age.

Dimension	Setting	Category 1, n (%)	Category 2, n (%)	Valid n
Time of day	Indoor	Daytime 10 (8.0)	Night 115 (92.0)	125
Time of day	Transport	Daytime 18 (39.1)	Night 28 (60.9)	46
Time of day	Outdoor	Daytime 24 (80.0)	Night 6 (20.0)	30
Gender	Indoor	Male 62 (50.0)	Female 62 (50.0)	124
Gender	Transport	Male 47 (92.2)	Female 4 (7.8)	51
Gender	Outdoor	Male 26 (70.3)	Female 11 (29.7)	37
Age	Indoor	Children 75 (44.9)	Adults 92 (55.1)	167
Age	Transport	Children 2 (3.2)	Adults 60 (96.8)	62
Age	Outdoor	Children 16 (40.0)	Adults 24 (60.0)	40

Note: percentages are computed within each setting using valid cases. Time × setting: $\chi^2 = 70.87$, df = 2, V = 0.594; gender × setting: $\chi^2 = 28.61$, df = 2, V = 0.367; age × setting: $\chi^2 = 35.34$, df = 2, V = 0.362; all $p < 0.001$. The age test merges ages ≥ 15 years into adults.

3.5 Cascading pathway from rainfall triggering to fatality consequence

Linking rainfall events with individual records through Event_ID and retaining only individuals whose triggering pattern, time of day, setting, age and gender are all explicit yields 145 victims and 32 complete combination paths (Fig. 7). Type D contributes 92 individuals and is the largest starting node in the complete sample; night, indoor, adult and male constitute the main nodes in the subsequent dimensions. The emphasis of the figure is not deterministic causation but how different triggering backgrounds co-occur with specific social settings. Because

https://doi.org/10.5194/egusphere-2026-6563
Preprint. Discussion started: 5 November 2026
© Author(s) 2026. CC BY 4.0 License.

310 complete cases cover only 46.9% of all victims, flow widths cannot be extrapolated to national population risk rates.

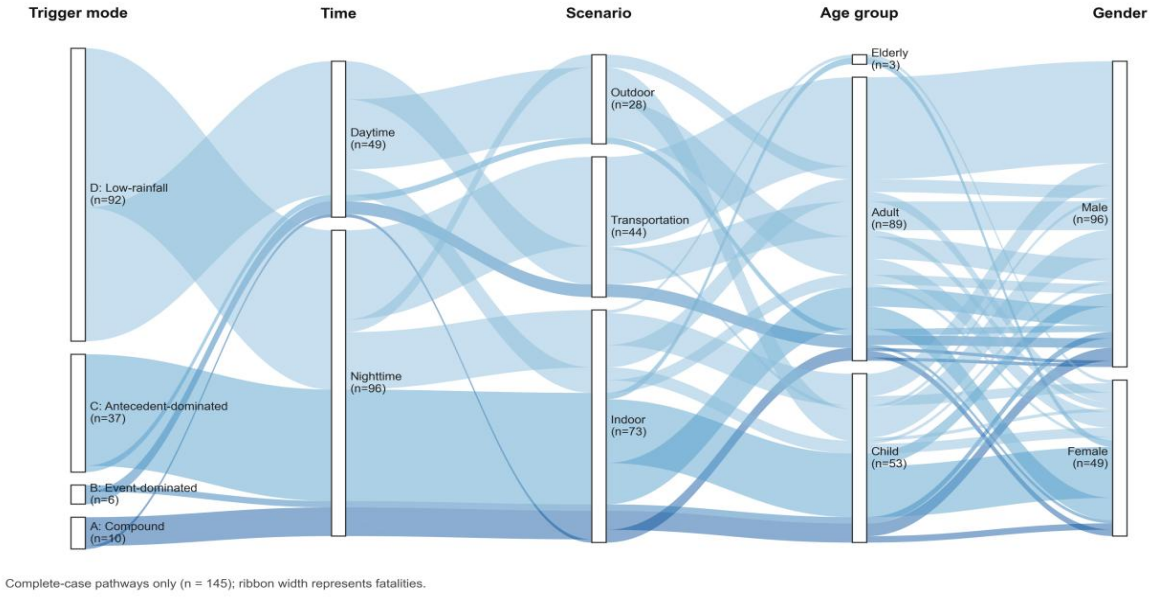


Fig. 7. Cascading flows among antecedent rainfall pattern, time of death, exposure setting, age group and gender. Band width indicates the number of deaths in the complete individual records (n = 145), and colours correspond to triggering-
315 pattern types A–D.

Two well-documented events illustrate this scenario-based relationship. The 2021 Gatka Imlok Bahri event (PKRFL-218) occurred at night, with P0 = 12.33 mm and AP7 = 64.05 mm, belonging to type C with a strongly wet antecedent state; the mudflow destroyed a dwelling and killed 13 family members. The 2023 Kuz Kalay event (PKRFL-228) had P0 = 10.76 mm and AP7 = 0 mm, belonging to type D; eight boys aged 7–14 years were buried
320 by the collapse of a sandy slope while playing outdoors. These two cases show that low P0 does not imply low consequence, and that different slope conditions and exposure scenarios can translate different rainfall backgrounds into mass casualties.

4 Discussion

4.1 “Zero event-day rainfall” should be regarded as an observation and process issue

325 That P0 is zero for more than half of the events is one of the most striking findings of this study, but it cannot be simply equated with “landslides occurring without rainfall”. CHIRPS uses UTC day boundaries, whereas Pakistan

https://doi.org/10.5194/egusphere-2026-6563
Preprint. Discussion started: 5 November 2026
© Author(s) 2026. CC BY 4.0 License.

local time differs by 5 h; news report dates may correspond to the time of discovery or rescue; and the 0.05° grid also smooths local mountain convection. More importantly, pore-water pressure response and deep seepage are lagged. Early-warning systems that monitor only the event day or short-duration rain intensity may therefore miss failures that occur after antecedent wetting. The absence of significant differences in AP7 and AP30 between the two P0 groups supports treating the period around the event day as a continuous hydrological process rather than making a binary judgement from a single-day value (Stanley et al., 2025; Noi et al., 2026).

In terms of the composition of zero values, zero event-day rainfall is not an isolated phenomenon: among the 213 level I–II events, P0 = 0 accounts for 53.5% (114 events), whereas the zero-value proportions of AP3, AP7 and Total_7d drop sharply to 17.8%, 10.3% and 8.5%, indicating that the great majority of events still experienced substantial rainfall within the week before occurrence. Wilcoxon rank-sum tests of antecedent cumulative rainfall between the P0 = 0 (n = 114) and P0 > 0 (n = 99) groups show no significant difference for either AP7 ($p = 0.523$) or AP30 ($p = 0.526$), further demonstrating that whether rainfall is recorded on the event day does not distinguish its antecedent wetness background. Seasonally, the proportion of P0 = 0 in the monsoon season (57.0%) is in fact higher than in the pre-monsoon season (48.3%) and winter (45.2%), contrary to the intuition that the heavy-rain season is dominated by immediate triggering, indicating that antecedent saturation–delayed triggering is widespread across seasons in Pakistan. The underlying reason is that intense tectonic activity in the northern high mountains has left the rock mass extremely fractured, and the interaction between abundant antecedent runoff infiltration and weak rock and soil is sufficient to dominate delayed slope failure (Iverson, 2000; Mirus et al., 2020).

4.2 Multiple rainfall backgrounds require season-specific warning criteria

The A–D classification shows that no single rainfall combination precedes fatal landslides in Pakistan. The proportion of high event-day-rainfall types is relatively high in the monsoon season, whereas the pre-monsoon season and winter show more low-P0 types, which may be related to the compound hydro-meteorological background formed by monsoon moisture, western disturbances and snowmelt in the high mountains. The main value of the empirical partition is to convert continuous rainfall variables into antecedent-rainfall scenarios that are easy to compare and communicate. The sensitivity analysis shows that under all three boundary sets (15/40, 20/50 and 25/60 mm), types C + D dominate, indicating that the conclusion that low event-day-rainfall types dominate is robust. These boundaries are not, however, universal physical critical values and cannot be used directly to issue warnings. Future work should calibrate separately for different climatic zones, slope types and seasons, and introduce non-landslide rainfall samples and independent validation sets to evaluate hit and false-alarm rates.

https://doi.org/10.5194/egusphere-2026-6563
Preprint. Discussion started: 5 November 2026
© Author(s) 2026. CC BY 4.0 License.

International experience also shows that even in densely observed regions, warning systems based solely on critical rainfall achieve a recall of only about 0.49 for fatal landslide events, and that many events occur under antecedent wetness backgrounds that did not exceed the critical rainfall (Kaihara et al., 2023), further indicating that a single threshold and short-duration monitoring are insufficient to cover multiple rainfall backgrounds.

Statistical tests of seasonal differences further support the above understanding: seasons differ significantly in AP7 ($\chi^2 = 10.08$, $p = 0.0179$) and AP30 ($\chi^2 = 14.08$, $p = 0.0028$), whereas the seasonal difference in event-day P0 is not significant ($p = 0.130$); that is, the seasonality of fatal landslides in Pakistan is expressed mainly in the antecedent cumulative wetness background rather than in same-day rain intensity. Spatially, the antecedent background is significantly higher on the windward slopes of Azad Kashmir (mean AP30 = 176.5 mm) and Khyber Pakhtunkhwa (140.4 mm) than in Gilgit–Baltistan (35.6 mm), which lies in a high-mountain rain shadow; the latter nevertheless records fatal events under low antecedent rainfall, suggesting that it is more likely controlled jointly by short-duration local rainfall, snowmelt or glacier ablation. Therefore, the bimodal pattern of a “monsoon main peak plus pre-monsoon secondary peak” and the differences in climatic background among regions together indicate that a single fixed national threshold is not robust, and that warnings should be calibrated by level, region and season (Guzzetti et al., 2008; Haque et al., 2019).

4.3 From hazard towards situational vulnerability

This study finds no significant association between rainfall metrics and the number of deaths in an individual event, indicating that the hydro-meteorological background of slope instability and the human fatality consequence belong to different links of the disaster chain. The concentration of deaths in the night–indoor setting reflects the superposition of sleeping state, difficulty in receiving warnings, fragile dwelling structures and shared household exposure; the strong concentration of transport deaths among adult males more likely reflects functional exposure arising from dependence on mountain roads and from the division of driving and labour; and the relatively high share of children among indoor and outdoor deaths may be related to children's hazard recognition, their capacity for independent evacuation and their activity spaces. This is consistent with the global understanding that disaster consequences are modulated by social conditions (Salvati et al., 2018; Pollock and Wartman, 2020; Gamperl et al., 2023; Li et al., 2026).

Placing natural triggering and individual consequence within a single visual framework is the main contribution of this paper relative to separate rainfall analysis or separate victim profiling. The cascading relations are, however,

https://doi.org/10.5194/egusphere-2026-6563
Preprint. Discussion started: 5 November 2026
© Author(s) 2026. CC BY 4.0 License.

observational co-occurrences and cannot prove that a given rainfall type necessarily causes death in a given population group. Their policy significance lies in identifying intervenable intermediate links: community alerts and pre-emptive evacuation targeted at night-time dwellings, temporary control of mountain roads during heavy rainfall, and slope inspection of children's activity areas at schools and settlement margins are all more targeted than issuing a uniform rainfall threshold. This study therefore does not treat rainfall and human vulnerability as two independent problems, but understands them as different links in the disaster chain: rainfall provides the hydro-meteorological background for slope instability, while the timing of the event, the exposed space and demographic attributes further modulate the conversion of a failure event into human fatalities.

Spearman rank correlation between rainfall metrics and fatality count shows that the coefficients for P0, AP3, AP7, AP15, AP30 and Total_7d are all weak and non-significant ($p > 0.05$), with AP3 the highest ($\rho = 0.103$, $p = 0.133$) and P0 almost unrelated ($\rho = -0.015$, $p = 0.825$), quantitatively confirming the judgement that "rainfall determines whether and when a landslide occurs, whereas who dies depends on exposure and vulnerability". In terms of setting structure, the night–indoor quadrant is the most lethal unit (115 individuals, accounting for 92.0% of the valid indoor sample), males account for 92.2% of transport-setting deaths, and children account for 44.9% of indoor-setting deaths and 40.0% of outdoor-setting deaths; the chi-square tests for gender × setting ($\chi^2 = 28.609$, $p = 0.0001$, Cramér's $V = 0.367$) and age × setting ($\chi^2 = 35.34$, $p = 0.0001$, $V = 0.362$) are both highly significant, indicating that exposure of population groups across settings is not random but structurally differentiated (Neumayer and Plümper, 2007; Shinohara and Kume, 2022). In terms of the cascade, type C (antecedent saturation–delayed triggering) flows mainly into the night–indoor node and causes family group casualties, whereas type B (sudden rainstorm) is more often routed to daytime–outdoor/transport and to adult males in transit or at work, suggesting that differentiated social interventions are more effective than a uniform rainfall threshold.

4.4 Uncertainty and research boundaries

This study has four limitations. First, news reports and public databases may omit remote areas, small events and some individual attributes, so the catalogue should be regarded as a lower-bound estimate. In data-scarce mountain regions, treating a catalogue as a "lower-bound estimate" is a common constraint, consistent with the situation of existing studies in areas such as northern Pakistan (Ullah et al., 2024). Second, the location error of level II events can reach tens of kilometres, which may introduce bias when matched to the roughly 5 km CHIRPS rainfall grid; daily data also cannot resolve hourly rainfall peaks, so low or zero P0 values must be interpreted with caution. Third, the P0/AP7 classification boundaries are used only for within-sample scenario partitioning and do not

https://doi.org/10.5194/egusphere-2026-6563
Preprint. Discussion started: 5 November 2026
© Author(s) 2026. CC BY 4.0 License.

represent physical triggering thresholds; although the sensitivity analysis supports the main conclusions, different boundaries still change the specific composition of each type. Fourth, the I–D quantile relations are established only from the fatal-event sample, lacking non-landslide rainfall and an independent validation set, so they cannot be used directly as operational warning thresholds; individual records are concentrated after 2018 and some attributes are missing, so the statistical relations and cascading paths should not be given a causal interpretation. Future work should introduce ground stations, radar or hourly satellite rainfall, establish event and non-event controls, and add variables such as housing, occupation, warning accessibility and behavioural response.

The sample control of this study also determines the boundaries of applicability of the conclusions. The 213 events used for event-by-event rainfall extraction are all of spatial accuracy levels I–II (85.2% of all 250 events); the 37 level III events with location errors exceeding 50 km were excluded because of substantial grid-matching error. This avoids amplification of error in rainfall extraction by low-accuracy locations, but it also means that the conclusions concern regional statistical regularities rather than precise values for individual events. At the individual level, in the 2018–2024 subset the identifiable proportions of gender, age group, fatality setting and time of day are 68.6%, 87.4%, 97.1% and 66.0%, respectively; the missing attributes are related to brief news reporting and incomplete post-disaster information disclosure, a limitation common to global landslide catalogue studies (Froude and Petley, 2018; Sultana, 2020; Görüm and Fidan, 2021). This study therefore retains the “unknown” category in overall statistics and uses only complete cases with all fields present in cross-analyses, in order to balance realism and robustness.

5 Conclusions

Based on 213 events with high spatial accuracy and records of 309 victims, this study shows that rainfall-induced fatal landslides in Pakistan are characterised by multiple antecedent rainfall backgrounds and pronounced situational vulnerability. P0 is zero in the CHIRPS daily record for 53.5% of events; under the baseline classification scheme the low-P0 types C + D account for 86.4%, and the sensitivity analysis shows that this conclusion is robust to reasonable adjustment of the classification boundaries. The I–D quantile relations of the fatal-event sample share a common exponent of −0.59, yet rainfall metrics at all timescales show no significant correlation with the number of deaths in an individual event, indicating that rainfall can describe the hydro-meteorological background of slope instability but cannot alone explain fatality magnitude. Victim records show that the night–indoor combination, adult males in transport settings, and children in indoor and outdoor settings constitute the most prominent exposure combinations. Early-warning systems should therefore attend to both short-

https://doi.org/10.5194/egusphere-2026-6563
Preprint. Discussion started: 5 November 2026
© Author(s) 2026. CC BY 4.0 License.

duration and antecedent cumulative rainfall, and translate warnings into scenario-based actions such as night-time evacuation of dwellings, mountain road control and management of children's activity spaces. The "rainfall background – time of day – setting – population group" framework proposed here can provide a reference for landslide risk governance oriented to human exposure settings in data-scarce mountain regions. This conclusion corroborates the global-scale understanding that socio-economic factors govern fatality risk (Fidan et al., 2026; Li et al., 2026). Compared with existing research in Pakistan, this study goes beyond the macro-level discussion of Shabbir et al. (2023) based on monthly TRMM data: through event-by-event, multi-window rainfall extraction it demonstrates the prevalence of "delayed triggering under an antecedent wetness background" among fatal landslides in Pakistan, and drills down to the level of individual profiling to reveal the decisive role of micro spatiotemporal situations (night–indoor, adult males in transport settings, children in indoor and outdoor settings) in fatal outcomes. It should be noted that these conclusions should be understood within the boundary conditions of catalogue completeness, the limits of daily rainfall data in observing short-duration rainfall peaks, and the fact that individual records cover only 2018–2024; future research could introduce hourly rainfall observations, event and non-event control samples, and variables such as housing and warning accessibility, to test the framework proposed here over longer time series and in other data-scarce mountain regions.

Compared with frontier work at the global scale, the increment of this paper lies in bringing the understanding that "consequences are modulated by social conditions" down to the event-scale rainfall–exposure chain. Li et al. (2026) reveal an "unexpected spatial inequality" in fatal landslide impacts at the global scale, the core of which is the spatial differentiation of population-normalised risk; this paper further demonstrates within a unified national catalogue that, even under the same regional rainfall background, fatality magnitude cannot be explained by rainfall metrics in any time window, indicating that consequence inequality exists not only in the spatial dimension but also in the dimension of "exposure differences under the same rainfall conditions". Fidan et al. (2026) attribute landslide fatalities on world mountains to wealth level and land-cover change; in mountain regions lacking gridded socio-economic data, this paper offers an operational alternative through the "rainfall background – time of day – setting – population group" framework, translating macro-level attribution into scenario-based interventions such as night-time evacuation of dwellings, mountain transport control and management of children's activity spaces.

Data availability

The 2004–2024 catalogue of rainfall-induced fatal landslides in Pakistan used in this study (250 events, 2073 fatalities), the three-level spatial accuracy grading results and the event-by-event CHIRPS rainfall metrics are

https://doi.org/10.5194/egusphere-2026-6563
Preprint. Discussion started: 5 November 2026
© Author(s) 2026. CC BY 4.0 License.

archived on Zenodo together with the companion data paper (Bai et al., 2026c, under review), DOI: 10.5281/zenodo.XXXXXXX (to be replaced by the permanent DOI upon publication). CHIRPS daily rainfall data are publicly available through Google Earth Engine (Funk et al., 2015; Gorelick et al., 2017). Individual-level victim records are released only as aggregated attributes of gender, age group, exposure setting and time of day.

Author contributions

SB conceived and designed the study. WZ compiled the catalogue, performed the statistical analyses and drafted the manuscript. XW contributed to data processing, rainfall extraction and figure preparation. PZ contributed to the interpretation of the results and to critical revision of the manuscript. All authors read and approved the final manuscript.

Competing interests

The authors declare that they have no competing interests.

Acknowledgements

This work was supported by the National Key Research and Development Program of China (grant no. 2023YFC3007200).

References

Bai, S., Wang, J., Thiebes, B., Cheng, C., Yang, Y., 2013. Analysis of the relationship of landslide occurrence with rainfall: a case study of Wudu County, China. Arabian Journal of Geosciences, 7(4), 1277–1285. https://doi.org/10.1007/s12517-013-0939-9

Brunetti, M.T., Melillo, M., Peruccacci, S., Ciabatta, L., Brocca, L., 2018. How far are we from the use of satellite rainfall products in landslide forecasting? Remote Sensing of Environment, 210, 65–75. https://doi.org/10.1016/j.rse.2018.03.016

Caine, N., 1980. The Rainfall Intensity - Duration Control of Shallow Landslides and Debris Flows. Geografiska Annaler: Series A, Physical Geography, 62(1-2), 23–27. https://doi.org/10.1080/04353676.1980.11879996

Champati ray, P.K., Dimri, S., Lakhera, R.C., Sati, S., 2007. Fuzzy-based method for landslide hazard assessment in active seismic zone of Himalaya. Landslides, 4(2), 101–111. https://doi.org/10.1007/s10346-006-0068-6

Chikalamo, E.E., Mavrouli, O.C., Ettema, J., van Westen, C.J., Muntohar, A.S., Mustofa, A., 2020. Satellite-derived rainfall thresholds for landslide early warning in Bogowonto Catchment, Central Java, Indonesia. International Journal of Applied Earth Observation and Geoinformation, 89. https://doi.org/10.1016/j.jag.2020.102093

Corominas, J., van Westen, C., Frattini, P., Cascini, L., Malet, J.P., Fotopoulou, S., Catani, F., Van Den Eeckhaut, M., Mavrouli, O., Agliardi, F., Pitilakis, K., Winter, M.G., Pastor, M., Ferlisi, S., Tofani, V., Hervás, J., Smith, J.T., 2014.

https://doi.org/10.5194/egusphere-2026-6563
Preprint. Discussion started: 5 November 2026
© Author(s) 2026. CC BY 4.0 License.

Recommendations for the quantitative analysis of landslide risk. Bulletin of Engineering Geology and the Environment, 73(2), 209–263. https://doi.org/10.1007/s10064-013-0538-8

Crozier, M.J., 1999. Prediction of rainfall-triggered landslides: a test of the Antecedent Water Status Model. Earth Surface Processes and Landforms, 24(9), 825–833. https://doi.org/10.1002/(SICI)1096-9837(199908)24:9<825::AID-ESP14>3.0.CO;2-M

Emberson, R., Kirschbaum, D.B., Amatya, P., Tanyas, H., Marc, O., 2022. Insights from the topographic characteristics of a large global catalog of rainfall-induced landslide event inventories. Nat. Hazards Earth Syst. Sci., 22(3), 1129–1149. https://doi.org/10.5194/nhess-22-1129-2022

Fidan, S., Görüm, T., Akbaş, A., Ekberzade, B., Ozturk, U., 2026. Wealth and land-cover change govern landslide fatalities on world's mountains. Science Advances, 12(15), eaec2739. https://doi.org/10.1126/sciadv.aec2739

Froude, M.J., Petley, D.N., 2018. Global fatal landslide occurrence from 2004 to 2016. Nat. Hazards Earth Syst. Sci., 18(8), 2161–2181. https://doi.org/10.5194/nhess-18-2161-2018

Funk, C., Peterson, P., Landsfeld, M., Pedreros, D., Verdin, J., Shukla, S., Husak, G., Rowland, J., Harrison, L., Hoell, A., Michaelsen, J., 2015. The climate hazards infrared precipitation with stations—a new environmental record for monitoring extremes. Scientific Data, 2(1), 150066. https://doi.org/10.1038/sdata.2015.66

Gamperl, M., Singer, J., Garcia-Londoño, C., Seiler, L., Castañeda, J., Cerón-Hernandez, D., Thuro, K., 2023. Recommendations for Landslide Early Warning Systems in Informal Settlements Based on a Case Study in Medellín, Colombia. Land, 12(7), 1451. https://doi.org/10.3390/land12071451

Gariano, S.L., Guzzetti, F., 2016. Landslides in a changing climate. Earth-Science Reviews, 162, 227–252. https://doi.org/10.1016/j.earscirev.2016.08.011

Glade, T., Crozier, M., Smith, P., 2000. Applying Probability Determination to Refine Landslide-triggering Rainfall Thresholds Using an Empirical "Antecedent Daily Rainfall Model". pure and applied geophysics, 157(6), 1059–1079. https://doi.org/10.1007/s000240050017

Gorelick, N., Hancher, M., Dixon, M., Ilyushchenko, S., Thau, D., Moore, R., 2017. Google Earth Engine: Planetary-scale geospatial analysis for everyone. Remote Sensing of Environment, 202, 18–27. https://doi.org/10.1016/j.rse.2017.06.031

Görüm, T., Fidan, S., 2021. Spatiotemporal variations of fatal landslides in Turkey. Landslides, 18(5), 1691–1705. https://doi.org/10.1007/s10346-020-01580-7

Guzzetti, F., 2000. Landslide fatalities and the evaluation of landslide risk in Italy. Engineering Geology, 58(2), 89–107. https://doi.org/10.1016/S0013-7952(00)00047-8

Guzzetti, F., Peruccacci, S., Rossi, M., Stark, C.P., 2008. The rainfall intensity–duration control of shallow landslides and debris flows: an update. Landslides, 5(1), 3–17. https://doi.org/10.1007/s10346-007-0112-1

Haque, U., Blum, P., da Silva, P.F., Andersen, P., Pilz, J., Chalov, S.R., Malet, J.-P., Auflič, M.J., Andres, N., Poyiadji, E., Lamas, P.C., Zhang, W., Peshevski, I., Pétursson, H.G., Kurt, T., Dobrev, N., García-Davalillo, J.C., Halkia, M., Ferri, S., Gaprindashvili, G., Engström, J., Keellings, D., 2016. Fatal landslides in Europe. Landslides, 13(6), 1545–1554. https://doi.org/10.1007/s10346-016-0689-3

Haque, U., da Silva, P.F., Devoli, G., Pilz, J., Zhao, B., Khaloua, A., Wilopo, W., Andersen, P., Lu, P., Lee, J., Yamamoto, T., Keellings, D., Wu, J.-H., Glass, G.E., 2019. The human cost of global warming: Deadly landslides and their triggers (1995–2014). Science of The Total Environment, 682, 673–684. https://doi.org/10.1016/j.scitotenv.2019.03.415

Huang, Y., Li, L., Xu, C., Cheng, J., Xu, X., Zheng, T., Zhang, X., 2022. Spatiotemporal distribution patterns of deadly geohazard events in China, 2013–2019. Natural Hazards Research, 2(4), 316–324. https://doi.org/10.1016/j.nhres.2022.10.003

Hungr, O., Leroueil, S., Picarelli, L., 2014. The Varnes classification of landslide types, an update. Landslides, 11(2), 167–194. https://doi.org/10.1007/s10346-013-0436-y

Iverson, R.M., 2000. Landslide triggering by rain infiltration. Water Resources Research, 36(7), 1897–1910. https://doi.org/10.1029/2000WR900090

Kaihara, S., Tadakuma, N., Saito, H., Nakaya, H., 2023. Influence of below-threshold rainfall on landslide occurrence based on Japanese cases. Natural Hazards, 115(3), 2307–2332. https://doi.org/10.1007/s11069-022-05639-7

Kirschbaum, D., Kapnick, S.B., Stanley, T., Pascale, S., 2020. Changes in Extreme Precipitation and Landslides Over High Mountain Asia. Geophysical Research Letters, 47(4), e2019GL085347. https://doi.org/10.1029/2019GL085347

https://doi.org/10.5194/egusphere-2026-6563
Preprint. Discussion started: 5 November 2026
© Author(s) 2026. CC BY 4.0 License.

Kirschbaum, D., Stanley, T., Zhou, Y., 2015. Spatial and temporal analysis of a global landslide catalog. Geomorphology, 249, 4–15. https://doi.org/10.1016/j.geomorph.2015.03.016

Kirschbaum, D.B., Adler, R., Hong, Y., Hill, S., Lerner-Lam, A., 2010. A global landslide catalog for hazard applications: method, results, and limitations. Natural Hazards, 52(3), 561–575. https://doi.org/10.1007/s11069-009-9401-4

Li, Z., Qiu, H., Petley, D., Liu, Y., Zhao, K., Yang, G., Song, J., Yang, D., 2026. Unexpected spatial inequality of fatal landslide impacts. Communications Earth & Environment. https://doi.org/10.1038/s43247-026-03850-z

Lin, Q., Wang, Y., 2018. Spatial and temporal analysis of a fatal landslide inventory in China from 1950 to 2016. Landslides, 15(12), 2357–2372. https://doi.org/10.1007/s10346-018-1037-6

Mancino, S., Sblano, A., Lovergine, F.P., Massimi, V., Sethi, T., Capolongo, D., Amatulli, G., 2026. Unified Global Landslide Catalogue (UGLC): a single, standardised global-scale landslide dataset. Earth Syst. Sci. Data, 18(7), 4697–4723. https://doi.org/10.5194/essd-18-4697-2026

Mirus, B.B., Jones, E.S., Baum, R.L., Godt, J.W., Slaughter, S., Crawford, M.M., Lancaster, J., Stanley, T., Kirschbaum, D.B., Burns, W.J., Schmitt, R.G., Lindsey, K.O., McCoy, K.M., 2020. Landslides across the USA: occurrence, susceptibility, and data limitations. Landslides, 17(10), 2271–2285. https://doi.org/10.1007/s10346-020-01424-4

Neumayer, E., Plümper, T., 2007. The Gendered Nature of Natural Disasters: The Impact of Catastrophic Events on the Gender Gap in Life Expectancy, 1981–2002. Annals of the Association of American Geographers, 97(3), 551–566. https://doi.org/10.1111/j.1467-8306.2007.00563.x

Ning, S., Ge, Y., Bai, S., Ma, C., Sun, Y., 2023. I–D Threshold Analysis of Rainfall-Triggered Landslides Based on TRMM Precipitation Data in Wudu, China. Remote Sensing, 15(15). https://doi.org/10.3390/rs15153892

Noi, D.T., Son, N.H., Thuy, D.T., Nga, N.T., Phuong, T.T., 2026. Long-Term Evaluation of Satellite Precipitation Products for Extreme Rainfall and Water-Related Hazard Assessment Along a Mountainous Corridor in Northern Vietnam. Water, 18(15), 1922. https://doi.org/10.3390/w18151922

Petley, D., 2012. Global patterns of loss of life from landslides. Geology, 40(10), 927–930. https://doi.org/10.1130/G33217.1

Petley, D.N., Hearn, G.J., Hart, A., Rosser, N.J., Dunning, S.A., Oven, K., Mitchell, W.A., 2007. Trends in landslide occurrence in Nepal. Natural Hazards, 43(1), 23–44. https://doi.org/10.1007/s11069-006-9100-3

Pollock, W., Wartman, J., 2020. Human Vulnerability to Landslides. GeoHealth, 4(10), e2020GH000287. https://doi.org/10.1029/2020GH000287

Saha, S., Bera, B., 2024. Rainfall threshold for prediction of shallow landslides in the Garhwal Himalaya, India. Geosystems and Geoenvironment, 3(3), 100285. https://doi.org/10.1016/j.geogeo.2024.100285

Salvati, P., Petrucci, O., Rossi, M., Bianchi, C., Pasqua, A.A., Guzzetti, F., 2018. Gender, age and circumstances analysis of flood and landslide fatalities in Italy. Science of The Total Environment, 610-611, 867–879. https://doi.org/10.1016/j.scitotenv.2017.08.064

Sepúlveda, S.A., Petley, D.N., 2015. Regional trends and controlling factors of fatal landslides in Latin America and the Caribbean. Nat. Hazards Earth Syst. Sci., 15(8), 1821–1833. https://doi.org/10.5194/nhess-15-1821-2015

Shabbir, W., Omer, T., Pilz, J., 2023. The impact of environmental change on landslides, fatal landslides, and their triggers in Pakistan (2003–2019). Environmental Science and Pollution Research, 30(12), 33819–33832. https://doi.org/10.1007/s11356-022-24291-z

Shinohara, Y., Kume, T., 2022. Changes in the factors contributing to the reduction of landslide fatalities between 1945 and 2019 in Japan. Science of The Total Environment, 827, 154392. https://doi.org/10.1016/j.scitotenv.2022.154392

Spearman, C., 1904. The Proof and Measurement of Association between Two Things. The American Journal of Psychology, 15(1), 72–101. https://doi.org/10.2307/1412159

Stanley, T.A., Sutton, J.R.P., Vershel, R.S., Amatya, P.M., 2025. Better Satellite Precipitation Algorithms Slightly Improved Landslide Hazard Assessment. Journal of Applied Meteorology and Climatology, 64(10), 1379–1394. https://doi.org/10.1175/JAMC-D-25-0021.1

Sultana, N., 2020. Analysis of landslide-induced fatalities and injuries in Bangladesh: 2000-2018. Cogent Social Sciences, 6(1), 1737402. https://doi.org/10.1080/23311886.2020.1737402

Ullah, Y., Shafique, M., Yu, L., Shah, N.A., 2024. Landslides hazard, vulnerability and risk mapping in the data-poor region of northern Pakistan. Environmental Earth Sciences, 83(19), 560. https://doi.org/10.1007/s12665-024-11858-x

Wang, N., Lombardo, L., Gariano, S.L., Cheng, W., Liu, C., Xiong, J., Wang, R., 2021. Using satellite rainfall products to assess the triggering conditions for hydro-morphological processes in different geomorphological settings in China.

https://doi.org/10.5194/egusphere-2026-6563
Preprint. Discussion started: 5 November 2026
© Author(s) 2026. CC BY 4.0 License.



International Journal of Applied Earth Observation and Geoinformation, 102. https://doi.org/10.1016/j.jag.2021.102350

Zhang, S., Li, C., Peng, J., Zhou, Y., Wang, S., Chen, Y., Tang, Y., 2023. Fatal landslides in China from 1940 to 2020: occurrences and vulnerabilities. Landslides, 20(6), 1243–1264. https://doi.org/10.1007/s10346-023-02034-6

605